Available online at www.sciencedirect.com
SCIENCE DIRECT®
Bioorganic & Medicinal Chemistry 13 (2005) 4262–4268
Bioorganic & Medicinal Chemistry

# Correlation of LUMO localization with the α-amylase inhibition constant in a Tendamistat-based series of linear and cyclic peptides

Deborah L. Heyl,* Steve Fernandes, Leena Khullar, Jennifer Stephens, Elizabeth Blaney, Horacia Opang-Owusu, Benjamin Stahelin, Todd Pasko, Jana Jacobs, Danielle Bailey, Dennis Brown and Maria C. Milletti

*Department of Chemistry, Eastern Michigan University, Ypsilanti, MI 48197, USA*

Received 12 January 2005; revised 8 April 2005; accepted 11 April 2005
Available online 4 May 2005

**Abstract**—The glycosidase α-amylase is responsible for the hydrolysis of α(1→4) glycosidic linkages found in dietary starch as one means for controlling blood sugar level. The effect of α-amylase is detrimental, however, in the disease state diabetes mellitus, where blood glucose levels are elevated due to a biochemical defect. Inhibition of the enzyme's activity would reduce glucose absorption by the small intestine. Our objective was to develop small peptides based on essential binding elements of the natural protein inhibitor, Tendamistat. These smaller analogs may be better studied structurally and conformationally to help us understand molecular-level interactions. In addition, we have been able to correlate the activity of our compounds with the lowest unoccupied molecular orbital (LUMO) localization in energy-minimized conformations. The positive charge/LUMO of most active inhibitors is localized on the central Arg residue of the required triplet. This provides a predictive model for the design of active molecules.


## 1. Introduction

The detailed mechanism of action of α-amylase is a subject of intense investigation due to its medical relevance. Specifically, inhibition of glycolytic enzymes has been found to reduce postprandial blood glucose peaks in diabetics.[1] Potential applications in obesity also exist. Elucidation of the three-dimensional structure of α-amylases from several organisms has shown them to be remarkably conserved in topology and composed of three main domains.[1] The domains include a central $(\beta/\alpha)_8$-barrel (domain A) with an extended loop (domain B), which is inserted between $\beta_3$ and $\alpha_3$;[2–4] domain C contains a Greek motif.[5] Calcium and, in some species, chloride binding sites also exist.[5] A 3 nm-long crevice in the enzyme between domains A and B can accommodate five glucose residues, consistent with a five subsite model[6] with cleavage occurring between subsites three and four.[5] Both small and polymeric substrates appear to undergo hydrolysis at the same catalytic site(s).[6]

A tight-binding pseudo-irreversible inhibitor of mammalian α-amylases with a $K_i$ value of $9 \times 10^{-12}$ M, Tendamistat, has been reported in the literature.[7,8] It induces a slow, progressive, pH-independent inhibition of the enzyme.[8] This large inhibitor molecule is an extracellular protein consisting of 74 amino acids and is isolated from the fermentation broth of *Streptomyces* bacteria. It bears structural similarity to several other protein α-amylase inhibitors, many isolated from plant sources. In fact, its three-dimensional structure has been determined by X-ray crystallographic analysis and nuclear magnetic resonance spectroscopy.[9,10]

In addition, it has been found that this conformation is the same when the inhibitor interacts with porcine pancreatic amylase. Topographical changes are induced in the enzyme, but not the inhibitor, upon binding.[5] Tendamistat forms a 1:1 stoichiometric complex with the enzyme[8] and blocks the access of the natural substrate, glycogen, or starch. However, only 15 of the 74 amino acids in the inhibitor (four segments in the sequence, as shown below) actually interact directly with the enzyme binding site via hydrogen bonding and hydrophobic and electrostatic forces.[11]

*Keywords*: α-Amylase; Tendamistat; Inhibitor; Peptide.
* Correspondence author. Tel.: +1 734 487 2057; fax: +1 734 487 1496; e-mail: debbie.heyl-clegg@emich.edu

0968-0896/$ - see front matter © 2005 Elsevier Ltd. All rights reserved.
doi:10.1016/j.bmc.2005.04.019

Segment 1: $Tyr^{15}Trp^{18}Arg^{19}Tyr^{20}$

Segment 2: $Leu^{44}Tyr^{46}$

Segment 3: $Gln^{52}Ile^{53}Thr^{54}Thr^{55}$

Segment 4: $Asp^{58}Gly^{59}Tyr^{60}Ile^{61}Gly^{62}$

Segment 1, containing the triplet Trp-Arg-Tyr, is characteristic of this class of inhibitors and binds at the catalytic site, blocking the five central sugar binding subsites.[5] The positively-charged side chain of Arg is oriented between the aromatic side chains of Trp and Tyr and projected outward where it can interact at the active site. The triplet is believed to induce a $3_{10}$-helix in the bound conformation of the enzyme, and evidence suggests that $Tyr^{15}$ is essential for avidity to mammalian α-amylases.

Development of a smaller inhibitor would be beneficial for several reasons, including reduction in immunogenecity and expense/difficulty of synthesis. In addition, shorter sequences are more easily studied structurally and more readily modeled. Dynamic energy minimization can be performed on a reasonable timescale. This may allow correlation of properties such as charge distribution or energy and location of valence orbitals with activity. Since detailed structural information is available for Tendamistat, it is an attractive target for the approach of general sequence minimization.

Small analogs of Tendamistat have been reported, notably cyclic hexapeptides containing the $Trp^{18}$-$Tyr^{20}$ or $Ser^{17}$-$Tyr^{20}$ template cyclized head-to-tail via amide bonds.[12,13] For the former, the triplet was constrained to a type I β-turn, as confirmed by NMR, and $K_i$ values ranged from 14 to 32 μM.[12] The Arg guanidinium side chain was found to be sandwiched between the aromatic rings of the adjacent residues in the essential loop, and these are believed to interact with specific groups in the active site of α-amylase. The analogs were designed to arrange these moieties in the appropriate orientation for interaction with the enzyme by using a properly chosen backbone scaffold. The peptide c(D-Pro-Phe-Ser-Trp-Arg-Tyr) gave a $K_i$ value of 14 μM, while the corresponding value for the replacement analog with Ala for Ser was 32 μM. Most linear tri- to hexapeptides bound with weaker affinity; the best, Ac-Trp-Arg-Tyr-OMe, acted as a competitive inhibitor with an inhibition constant of 100 μM.

In a parallel study, different backbone geometries were forced onto 15 analogs by varying the other two residues (generally Pro and Ala) of hexapeptides containing the $Ser^{17}$-$Tyr^{20}$ template, as well as their chirality and their placements within the cycle.[13] Hexapeptides were cyclized by lactam formation. Three of the 15 analogs were found to agree conformationally with the segment in Tendamistat, and some of the analogs demonstrated weak biological activity as α-amylase inhibitors, with $K_i$ values ranging from 120 to 277 μM. $Arg^{19}$ was found to be essential for activity.

In a similar study, Ono and co-workers synthesized six odd-length cyclic peptides and four even-length cyclic peptides containing the Trp-Arg-Tyr triplet of Tendamistat capped at both ends by Cys residues and cyclized via disulfide bonds. They reported $K_i$ values ranging from 0.27 to 1.41 μM, which increased with increasing peptide length.[14,15] They also prepared linear peptides corresponding to the cyclic peptides and reported that their inhibitory activities were comparable.

Our analogs were similar to those described above but take advantage of both the required Trp-Arg-Tyr (WRY) interaction sequence as well as vital surrounding residues (specifically, the $Tyr^{15}$, which is known to be vital for interaction with mammalian forms of the enzyme and $Gln^{22}$, also alleged to be important for binding).[11,15] In Tendamistat, this segment forms a bend or turn that projects the positively charged Arg side chain outward. Instead of capping the chain artificially with Cys residues, we replaced the native Ser positions with Cys due to their isosteric properties. Replacement of Ser with other residues was tolerated in other cyclic series,[12] since the influence of cyclization on conformation outweighed other potential advantageous interactions. Penicillamine (Pen, β,β-dimethycysteine) was also chosen to confer additional spatial limitations. Cyclization was accomplished by forming a disulfide bond between these internal Cys and/or Pen residues. Some analogs also contained a D-Pro inserted just after the triplet in an effort to induce a bend[13] in conformation. In the linear peptides, Ser was either retained or replaced with Ala to investigate the role of the serine side chain hydroxyl group, which is thought to form a conformation-stabilizing hydrogen bond.

## 2. Results and discussion

Our analogs were capped at the N-terminus with an acetyl group and at the C-terminus as a carboxamide in order to delete charges in the backbone. Sixteen peptide analogs based on Tendamistat were synthesized and purified (Compounds **NFH I–XVI** below in Table 1). These analogs retain the essential elements of segment 1 (Tyr-Trp-Arg-Tyr), which are found in all protein α-amylase inhibitors and provide the main site for interaction with the enzyme.[11] For **NFH I–VII**, cyclization via disulfide bond formation imposed a conformational constraint, which was hoped to lock the peptides into the optimal three-dimensional arrangement for enzyme interaction. The latter four analogs contained D-Pro, which has been shown to force a turn conformation in cyclic peptides. This addition also creates cyclic hexapeptides, which often adopt a dual turn topology.[12] For comparison, the analogous linear analogs (**NFH IX** and **XIII**) were tested where the native Ser was maintained. The requirement for the serine hydroxyl was examined by the synthesis and kinetic analysis of **NFH X–XII** and **NFH XIV–XVI**. This involved monitoring spectrophotometrically the increase in absorbance at 405 nm when *p*-nitrophenyl-α-D-maltoside was acted upon by porcine pancreatic α-amylase; *p*-nitrophenolate was liberated, giving a yellow color. The kinetic

**Table 1.** Sequences, average inhibitory constants and position of LUMO for peptide analogs

| NFH # | Sequence | $K_i \pm$ SEM (μM) | Location of LUMO |
|---|---|---|---|
| **I** | Ac-YQc(CWRYC)Q-$NH_2$ | Activation | Disulfide |
| **II** | Ac-YQc(CWRYPen)Q-$NH_2$ | Activation | N-terminal Tyr side chain |
| **III** | Ac-YQc(PenWRYC)Q-$NH_2$ | Activation | Disulfide/adjacent backbone |
| **IV** | Ac-YQc(PenWRYPen)Q-$NH_2$ | Activation | Backbone |
| **V** | Ac-YQc(CWRY-D-Pro-C)Q-$NH_2$ | 237 ± 51.6 | Arg side chain |
| **VI** | Ac-YQc(CWRY-D-Pro-Pen)Q-$NH_2$ | 990 ± 304 | Disulfide |
| **VII** | Ac-YQc(PenWRY-D-Pro-C)Q-$NH_2$ | 2010 ± 610 | Disulfide |
| **VIII** | Ac-YQc(PenWRY-D-Pro-Pen)Q-$NH_2$ | 4660 ± 1120 | Middle Tyr side chain |
| **IX** | Ac-YQSWRYSQ-$NH_2$ | 322 ± 41.6 | Arg side chain |
| **X** | Ac-YQAWRYSQ-$NH_2$ | 1550 ± 153 | Arg side chain |
| **XI** | Ac-YQSWRYAQ-$NH_2$ | 852 ± 102 | Arg side chain |
| **XII** | Ac-YQAWRYAQ-$NH_2$ | 517 ± 156 | Arg side chain |
| **XIII** | Ac-YQSWRY-D-Pro-SQ-$NH_2$ | 585 ± 41.3 | Arg side chain |
| **XIV** | Ac-YQAWRY-D-Pro-SQ-$NH_2$ | 112 ± 34.0 | Trp side chain |
| **XV** | Ac-YQSWRY-D-Pro-AQ-$NH_2$ | 242 ± 84.2 | Arg side chain |
| **XVI** | Ac-YQAWRY-D-Pro-AQ-$NH_2$ | 459 ± 128 | Arg side chain |

parameters were determined in the absence and presence of the inhibitor at three or more different inhibitor concentrations. The effect of peptide inhibitors on the kinetic parameters was used to determine the type of inhibition. Mean $V_{max}$ and $K_m$ values for α-amylase in our assay system were $1.06 \times 10^{-5}$ M/min and 10.0 mM, respectively. Each analog was then subjected to energy minimization and modeling by Spartan and Gaussian software. The localization and the energy of the LUMO were determined. Inhibition constants and location of the LUMO are provided in Table 1. Physiochemical data for the synthesized peptides are given in Table 2.

With the exception of **NFH V**, the cyclic analogs (**NFH I–VIII**) showed either very poor activity or, unexpectedly, slight activation. The incorporation of D-Pro in the sequence did not significantly enhance the inhibitory activity overall, but it did alter the effect on the enzyme and was apparently favorable in the Cys/Cys analog (**NFH I**, an activator, vs **NFH V**, the best inhibitor). Analogs containing Pen rather than Cys were weaker inhibitors, perhaps due to the additional conformational constraint imposed by the β-methyl groups (our theoretical energy-minimized structures, described below, revealed a slightly altered overall conformation for analogs containing Pen relative to those with Cys due to the steric effects). Kinetic analysis determined the mode of inhibition as competitive. Cyclization of the analogs did not result in notable inhibitory activity as had been hoped.

Visual observation provided clear qualitative evidence of enzyme inhibition for the linear analogs, as tubes containing the inhibitor were distinctively less yellow in color than the tubes without inhibitor. In some cases, we were able to achieve competitive enzyme inhibition in the milli-to-micromolar range (although we have lost orders of magnitude from the original Tendamistat) after minimizing the sequence. This has given us some

**Table 2.** Physicochemical properties of analogs

| NFH # | Sequence | Mol. Wt[a] | Purity[b] (%) | HPLC-1[c] | HPLC-2[d] |
|---|---|---|---|---|---|
| **I** | Ac-YQc(CWRYC)Q-$NH_2$ | 1189.5 | 98.1 | 0.85 | 0.67 |
| **II** | Ac-YQc(CWRYPen)Q-$NH_2$ | 1217.6 | 97.4 | 0.46 | 1.0 |
| **III** | Ac-YQc(PenWRYC)Q-$NH_2$ | 1217.3 | 97.9 | 0.56 | 0.93 |
| **IV** | Ac-YQc(PenWRYPen)Q-$NH_2$ | 1245.6 | 98.0 | 0.59 | 1.0 |
| **V** | Ac-YQc(CWRY-D-Pro-C)Q-$NH_2$ | 1284.6 | 98.9 | 0.69 | 0.78 |
| **VI** | Ac-YQc(CWRY-D-Pro-Pen)Q-$NH_2$ | 1312.7 | 98.5 | 0.81 | 1.0 |
| **VII** | Ac-YQc(PenWRY-D-Pro-C)Q-$NH_2$ | 1312.6 | 99.8 | 0.78 | 0.56 |
| **VIII** | Ac-YQc(PenWRY-D-Pro-Pen)Q-$NH_2$ | 1340.7 | 99.2 | 0.47 | 0.44 |
| **IX** | Ac-YQSWRYSQ-$NH_2$ | 1157.7 | 99.3 | 0.67 | 0.78 |
| **X** | Ac-YQAWRYSQ-$NH_2$ | 1141.8 | 99.3 | 0.81 | 0.89 |
| **XI** | Ac-YQSWRYAQ-$NH_2$ | 1141.6 | 99.7 | 0.77 | 0.78 |
| **XII** | Ac-YQAWRYAQ-$NH_2$ | 1125.7 | 99.2 | 0.89 | 1.0 |
| **XIII** | Ac-YQSWRY-D-Pro-SQ-$NH_2$ | 1254.7 | 99.5 | 0.81 | 0.70 |
| **XIV** | Ac-YQAWRY-D-Pro-SQ-$NH_2$ | 1238.7 | 99.0 | 0.96 | 0.89 |
| **XV** | Ac-YQSWRY-D-Pro-AQ-$NH_2$ | 1238.7 | 98.9 | 0.94 | 0.93 |
| **XVI** | Ac-YQAWRY-D-Pro-AQ-$NH_2$ | 1222.6 | 98.4 | 1.0 | 0.93 |

[a] Molecular weight obtained by liquid chromatography mass spectrometry.
[b] Purity of final product peptide as assessed by RP-HPLC peak integration at 214 or 230 nm (whichever is lower), utilizing a Waters C-18 (4.6 × 150 mm) column and a gradient of 0–66% aqueous acetonitrile over 22 min.
[c] $K'$ on reversed phase Waters C-18 HPLC (4.6 × 150 mm) column under 100% aqueous isocratic conditions.
[d] $K'$ on reversed phase Hewlett–Packard C-8 HPLC (4.6 × 250 mm) column under 100% aqueous isocratic conditions.

hope that smaller structures can retain some activity. The main focus within this group was the comparison of analogs containing native serine to those with alanine replacements. The modifications examined the role of hydrogen bonding by the serine in stabilizing the required conformation for enzyme interaction. Substitution of Ser was slightly detrimental for the analogs without D-Pro (**NFH IX–XII**), suggesting that hydrogen bonding is somewhat important in maintaining the three-dimensional bent shape for optimal interaction with the enzyme. This is not surprising since **NFH IX** is comprised of residues from Tendamistat's native sequence and might be expected to retain similar intramolecular interactions. Both the crystal structure and NMR of Tendamistat indicate the presence of a hydrogen bond between the $Ser^{17}$ side chain hydroxyl oxygen and the amide NH of $Tyr^{20}$, which is assumed to help stabilize the β-turn conformation of the triplet.[12] This particular Ser residue is also conserved in several members of the proteinaceous inhibitor family (in the one inhibitor where it is not, the position is an Asp, which may allow for the same interaction).[12] Our preliminary data also suggest the importance of the Ser residue in **NFH IX**, and this is consistent with results reported for similar linear hexapeptide analogs with Ser→Ala substitution.[12]

It should be noted that our theoretical energy-minimized structures for these smaller analogs differ conformationally in the triplet region from Tendamistat itself. Specifically, in almost all analogs, the Trp and Tyr aromatic side chains lie on the opposite side of the peptide backbone from the Arg side chain, which extends outward. This is true for both cyclic and linear peptides, although the overall topology of the cyclic analogs is dissimilar due to the conformational constraint imposed by the disulfide. Structures for most linear analogs indicate a possible hydrogen bond between the Arg guanidino group and either the first Ser, when present, or the adjacent peptide backbone. This variation in the H-bonding profile may contribute to the diversity in activity. This preliminary finding also suggests that the three side chains of the Trp-Arg-Tyr triplet should be on the same side of the backbone for maximal binding as in Tendamistat itself. Of course, the smaller analogs also lack the ability for extended contact with the enzyme away from the active site.

In comparing **NFH IX** to **NFH XIII**, it is clear that inserting D-Pro after the triplet is not favorable in the linear analogs. However, removal of the hydroxyl (Ala substitution for Ser) was actually favorable in **NFH XIV–XVI** containing the D-Pro insert (with Ala-containing analogs binding better than **NFH XIII**), suggesting a different intramolecular arrangement of atoms in these peptides. Ono et al.[14] proposed a second β-turn stabilizing hydrogen bond between $Tyr^{15}$ and $Gln^{22}$, which may be important in the maintenance of conformation for linear analogs, and insertion of D-Pro would be expected to shift these groups out of alignment. In this case, the Ser residues may present more of a disadvantage than the Ala since the polar hydroxyl group must be desolvated to bind at the active site.[12] In the theoretical structures, the conformations of the linear analogs containing D-Pro indeed differ from those lacking the residue in that the C-terminal portion of the backbone is forced upward toward the Arg side chain, resulting in some steric crowding and possible interactions with the Arg (a hydrogen bond between the guanidino group and the C-terminal Gln).

The unexpected result of enzyme activation for several of the analogs, as well as the wide range in inhibitory activity, led to our additional investigation of the energy and conformation of the molecules in an effort to explain the differential activity on the enzyme. The peptides were modeled and their structures optimized by the Spartan'02 software program[16]using the semi-empirical AM1 method.[17] Subsequently, the Gaussian'03 software program[18] was used to perform ab initio Hartree–Fock calculations[19] employing a 3-21G* basis set[20] on the molecular structures optimized at the AM1 level. The molecular wavefunction thus obtained was used to compute partial atomic charges using both the Mulliken[21] and Natural Bond Orbital[22] approximations; molecular orbital energies and surfaces (specifically, those of the LUMO); and an isosurface of the electrostatic potential mapped onto the total electron density.[23] Both Mulliken and natural atomic charges indicate that the arginine carbon carries the most positive partial charge in all analogs. Similarly, the electrostatic potential isosurfaces show a region of positive charge on the Arg residue of each analog. On the other hand, location of the LUMO surface is not the same for all analogs: it is localized over the important Arg residue only for the inhibitors, not for the analogs found to be activating (see Fig. 1). The only exception to this pattern is **NFH XIV**, where the LUMO is localized on the Trp side chain. However, the third lowest unoccupied orbital of this molecule (LUMO + 2) is localized on the Arg residue. This suggests that the LUMO should be localized on the positively charged Arg side chain for inhibition to occur. This makes sense since the Arg side chain guanidinium group projects outward from Tendamistat and interacts at the active site. Compounds in which the LUMO is found on other residues or moieties act as poor inhibitors and even activators, suggesting that they might interact at a different enzyme site. This study provides important information in the design of amylase blockers (where cyclization actually is detrimental), and additionally may be utilized to design pharmaceutical agents to treat the opposite ailment, hypoglycemia.

## 3. Conclusion

Twelve analogs reported here demonstrated visible evidence of inhibition, and $K_i$ values were determined ranging from 237 to 4660 μM. Competitive inhibition was demonstrated, which is indicative of interaction at the active site and consistent with the premise that the triplet is a key binding segment. In the cyclic series, most analogs were poor inhibitors; in fact, four of the cyclic analogs unexpectedly acted as slight activators of the enzyme. Side chain to side chain disulfide bond formation between internal positions generally did not result in

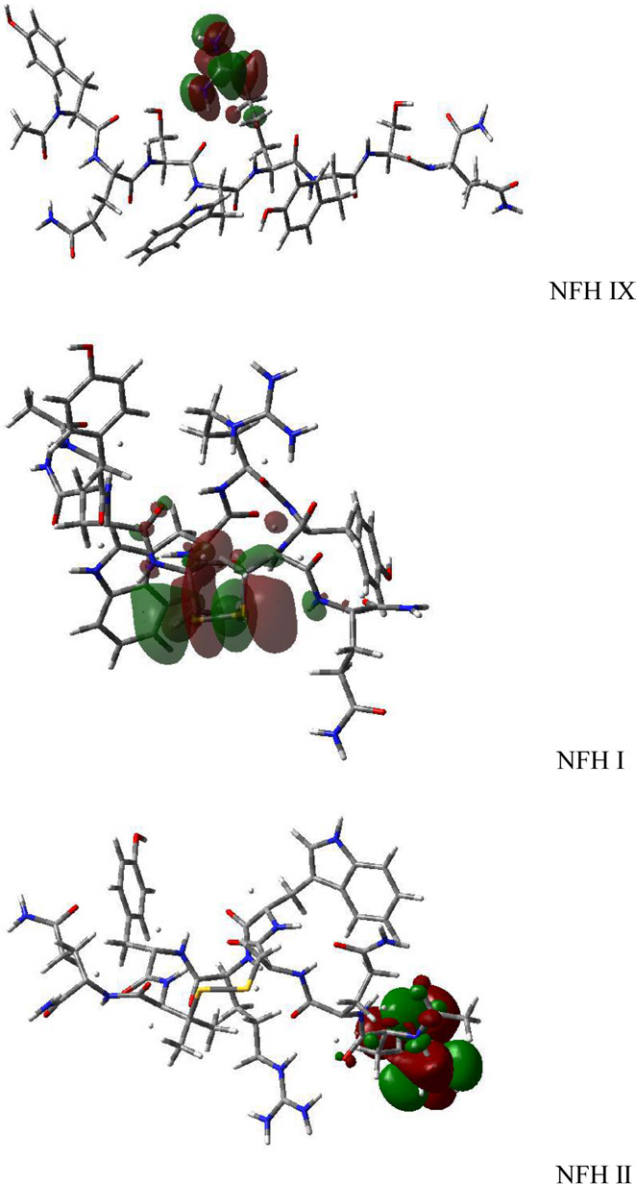


**Figure 1.** LUMO isosurfaces for three of the analogs; **NFH IX** (Arg side chain) **NFH I** (disulfide bond) and **NFH II** (N-terminal Tyr). Different surface colors represent opposite signs of the wavefunction. Analog structures are shown with a tube rendering; nitrogen atoms are in blue and oxygen atoms are in red.

potent inhibitors, but incorporation of D-Pro was favorable in the peptide containing two Cys residues. In the linear series, the native sequence demonstrated the best activity, and replacement of Ser with Ala was detrimental, suggesting the importance of the side chain hydroxyl. However, the same Ser→Ala replacement was favorable in analogs in which D-Pro was inserted after the Trp-Arg-Tyr triplet, most likely due to a different three-dimensional arrangement. Most active inhibitors, whether cyclic or linear, possessed a localization of the positive charge/LUMO on the central Arg residue of the required triplet. This provides a predictive model for the design of active molecules. Results of the calculations indicate that there is a correlation between the inhibiting power of the analogs and the position of the LUMO, while the position of the most positive charge appears to remain the same. This suggests that the interaction with the α-amylase enzyme is primarily orbital controlled, not charge controlled.

## 4. Experimental

### 4.1. Peptide synthesis

All protected amino acids were purchased from Bachem, Synthetech, and Protein Technologies. Coupling agents and resins were purchased from Bachem. Solvents and deprotecting agents were obtained from Fisher Scientific and Aldrich Chemical Co. The peptides were prepared on a PS3 Automated Peptide Synthesizer from Protein Technologies using standard solid phase techniques for *N*-α-fluorenylmethyloxycarbonyl (Fmoc) protected amino acids on Rink amide *p*-methylbenzhydrylamine (MBHA) resin (0.6 mmol/g). The side chains of Tyr, and Ser were protected as the *t*-butyl derivatives, and Arg was protected with the 2,2,5,7,8-pentamethylchroman-6-sulfonyl (Pmc) group. The deprotection solution for the N-terminal amine was 20% piperidine in *N*,*N*-dimethylformamide (DMF). *O*-(Benzotriazol-1-yl)-1,1,3,3-tetramethyluronium hexafluorophosphate (HBTU) was used as a coupling agent, activated by 0.4 M *N*,*N*-diisopropylethylamine (DIEA) in DMF. The N-terminal Fmoc group was removed, and acetylation was accomplished by treatment with acetic anhydride. Simultaneous deprotection and cleavage from the resin were accomplished by treatment with 11 mL 90% trifluoroacetic acid (TFA)/10% scavenger cocktail (anisole, thioanisole, phenol, water). The reaction was begun at 0 °C, allowed to warm to room temperature and stirred for 2 h. The uncharged resin was separated from the solution by filtration. The peptide was precipitated with cold diethyl ether, filtered, redissolved in 30% acetonitrile/70% water, and lyophilized. Crude peptides were purified to homogeneity by preparative reversed-phase high performance liquid chromatography (RP-HPLC) on a Waters instrument with a Phenomenex C18 column (2.2 × 25.0 cm, 10 mL/min). A linear gradient of 10% acetonitrile (0.1% TFA)/water (0.1% TFA) to 50% acetonitrile (0.1% TFA)/water (0.1% TFA) was employed, followed by lyophilization.

### 4.2. Peptide cyclization (analogs I–VII)

To 2 mL 5% carbon tetrachloride/methylene chloride was added 2 mg purified peptide and 13 μL 1 M tetrabutylammonium fluoride (TBAF) in tetrahydrofuran (THF). The reaction was stirred for 10 min, then quenched using 10 μL glacial acetic acid.[24] After evaporation of the solvent under nitrogen, cyclized peptide was dissolved in acetic acid, and purified using RP-HPLC, utilizing a gradient of 0–66% aqueous acetonitrile over 22 min. The absence of free sulfhydryl groups was confirmed with Ellman's test.[25]

### 4.3. Peptide analysis

Peptide purity was assessed by analytical RP-HPLC. Peaks were monitored at 214, 230, 254, and 280 nm.

All compounds were at least 97% pure as analyzed by peak integration. Proton nuclear magnetic resonance ($^1$H NMR) spectra were obtained on a Bruker spectrometer at 250 MHz. Samples (approximately 1 mg) were dissolved in DMSO. Diagnostic resonances and peak patterns confirmed the presence of all indicated residues. Liquid chromatography mass spectroscopy confirmed the appropriate molecular weights.

### 4.4. Kinetic assay

A spectrophotometric assay using a Beckman DU 246 spectrophotometer was used to determine inhibitory activity. *p*-Nitrophenyl-α-D-maltoside (*p*NPM, purchased from Calbiochem Corp) serves as a substrate for porcine pancreatic α-amylase (PPA, isozyme I, purchased from Sigma). During the reaction, 3.7% of the substrate is cleaved, with 59% of the cleavage occurring between the *p*-nitrophenyl group and the maltose unit.[6] Cleavage at the other position releases *p*-nitrophenyl glucose, which is a poor substrate and does not interfere with the reaction. The yellow *p*-nitrophenolate ion released upon cleavage (in equilibrium with *p*-nitrophenol) absorbs at 405nm. A solution of 0.025 M *N*-2-hydroxyethylpiperazine-*N*′-2-ethanesulfonic acid (HEPES) was used to buffer at pH 7.2. Stock solutions of substrate (50 mM, diluted to 0.1–20 mM per tube) and enzyme (51 μM, diluted to 1.5 μM per tube) were prepared in buffer solution and that of peptide inhibitors (0.6–30 mM) in dimethylsulfoxide (DMSO). An equal volume of DMSO was added to the reaction tubes without the inhibitor as a control solvent. Previous runs determined that the small volume of organic solvent did not influence the reaction. Reactions in the presence and absence of inhibitors were carried out simultaneously; inhibitor concentrations ranged from 0.1 to 5.0 mM. Enzyme and inhibitor were preincubated for 30 min at 30 °C. The reaction then was begun by the addition of substrate, and the initial rate of the reaction was recorded at 405 nm for three minutes. This absorbance-based rate was converted to a concentration-based initial velocity by multiplying by a conversion factor derived from Beer's Law. Kinetic analyses included the construction of Michaelis–Menten, Lineweaver–Burk, Eadie–Hofstee, and Hanes–Woolf plots with curve/line-fitting by Microsoft Excel. The inhibition constant ($K_i$) was determined as the mean (± standard error of the mean, SEM) of $K_i$ values determined from Lineweaver–Burk plots of individual runs, where the slopes of inhibited lines were shifted by a factor of $(1 + [I]/K_i)$, or, in some cases, as the negative x-intercept of the plot of the slopes of the Lineweaver–Burk plots against inhibitor concentration (in these latter cases, $K_i$ values were consistent between both methods of determination).

### 4.5. Molecular modeling

Each peptide was modeled using a two-step approach: the structure was first optimized using Spartan'02[16] at the semi-empirical AM1 level.[17] Use of semi-empirical calculations allowed for the geometry optimization to occur in a reasonable amount of time. Subsequently, Gaussian'03[18] was used to perform ab initio Hartree–Fock calculations[19] at the 3-21G* basis set level[20] on the optimized molecular structures. The molecular wavefunction thus obtained was used to obtain electronic characteristics for each analog, including Mulliken[21] and Natural[22] atomic charges; molecular orbital energies and surfaces (specifically, those of the LUMO); and an isosurface of the electrostatic potential mapped onto the total electron density.[23] There is precedent in the recent literature for using Hartree–Fock methods (HF) to obtain optimized structures of polypeptides.[26,27] In both papers, the basis set used in conjunction with the HF method was 6-31G*, but the authors were considering dipeptides only. Given the size of our peptides, the 3-21G* basis set is a more practical choice.

## Acknowledgements

Mass spectral analyses were provided by Dr. Hank Mosberg and colleagues at The University of Michigan College of Pharmacy. This work was supported by PRF grant #34911-B4 from the American Chemical Society and EMU Faculty Research Fellowship and Graduate School Support Awards.

## References and notes

1. Meyer, B. H.; Muller, F. O.; Kruger, J. B.; Grigoleit, H. G. *Lancet* **1983**, *1*, 934.
2. MacGregor, A.; Svensson, B. *Biochem. J.* **1989**, *259*, 145–152.
3. Qian, M.; Haser, R.; Payan, F. *J. Mol. Biol.* **1993**, *231*, 785–799.
4. Larson, S.; Greenwood, A.; Cascio, D.; Day, J.; McPherson, A. *J. Mol. Biol.* **1994**, *235*, 1560–1584.
5. Machius, M.; Vertesy, L.; Huber, R.; Wieland, G. *J. Mol. Biol.* **1996**, *260*, 409–421.
6. Seigner, C.; Prodanov, E.; Marchis-Mouren, G. *Eur. J. Biochem.* **1985**, *148*, 161–168.
7. Aschauer, H.; Vertesy, L.; Nesemann, G.; Braunitzer, G. *Hoppe-Seyler's Z. Physiol. Chem.* **1983**, *364*, 1347–1356.
8. Vertesy, L.; Odeing, V.; Bender, R.; Zepf, K.; Nesemann, G. *Eur. J. Biochem.* **1984**, *141*, 505–512.
9. Pflugrath, J. W.; Wiegand, G.; Huber, R.; Vertesy, L. *J. Mol. Biol.* **1986**, *189*, 383–386.
10. Kline, A. D.; Braun, W.; Wuthrich, K. *J. Mol. Biol.* **1988**, *204*, 675–724.
11. Wiegand, G.; Epp, O.; Huber, R. *J. Mol. Biol.* **1995**, *247*, 99–110.
12. Etzkorn, F.; Guo, T.; Lipton, M.; Goldberg, S.; Bartlett, P. *J. Am. Chem. Soc.* **1994**, *116*, 10412–10425.
13. Matter, H.; Kessler, H. *J. Am. Chem. Soc.* **1995**, *117*, 3347–3359.
14. Ono, S.; Hirano, T.; Yasutake, H.; Matsumoto, T.; Yamaura, I.; Kato, T.; Morita, H.; Fujii, T.; Yamazaki, I.; Shimasaki, C.; Yoshimura, T. *Biosci. Biotechnol. Biochem.* **1998**, *62*(8), 1621–1623.
15. Ono, S.; Umezaki, M.; Tojo, N.; Hashimoto, S.; Hiroko, T.; Kaneko, T.; Morita, H.; Fujii, T.; Yamazaki, I.; Shimasaki, C.; Yoshimura, T.; Kato, T. *J. Biochem.* **2001**, *129*, 783–790.
16. Spartan'02, Wavefunction Inc. Irvine CA.
17. (a) Dewar, M.; Thiel, W. *J. Am. Chem. Soc.* **1977**, *99*, 4499; (b) Davis, L. P. et al. *J. Comput. Chem.* **1981**, *2*, 433;

(c) Dewar, M. J. S.; McKee, M. L.; Rzepa, H. S. *J. Am. Chem. Soc.* **1978**, *100*, 3607; (d) Dewar, M. J. S.; Zoebisch, E. G.; Healy, E. F. *J. Am. Chem. Soc.* **1985**, *107*, 3902; (e) Dewar, M. J. S.; Jie, C.; Zoebisc, E. G. *Organometallics* **1988**, *7*, 513;; (f) Anders, E.; Koch, R.; Freunscht, P. *J. Comput. Chem.* **1993**, *14*, 1301.

18. Frisch, M. J.; Trucks, G. W.; Schlegel, H. B.; Scuseria, G. E.; Robb, M. A.; Cheeseman, J. R.; Montgomery, J. A.; Vreven, T., Jr; Kudin, K. N.; Burant, J. C.; Millam, J. M.; Iyengar, S. S.; Tomasi, J.; Barone, V.; Mennucci, B.; Cossi, M.; Scalmani, G.; Rega, N.; Petersson, G. A.; Nakatsuji, H.; Hada, M.; Ehara, M.; Toyota, K.; Fukuda, R.; Hasegawa, J.; Ishida, M.; Nakajima, T.; Honda, Y.; Kitao, O.; Nakai, H.; Klene, M.; Li, X.; Knox, J. E.; Hratchian, H. P.; Cross, J. B.; Adamo, C.; Jaramillo, J.; Gomperts, R.; Stratmann, R. E.; Yazyev, O.; Austin, A. J.; Cammi, R.; Pomelli, C.; Ochterski, J. W.; Ayala, P. Y.; Morokuma, K.; Voth, G. A.; Salvador, P.; Dannenberg, J. J.; Zakrzewski, V. G.; Dapprich, S.; Daniels, A. D.; Strain, M. C.; Farkas, O.; Malick, D. K.; Rabuck, A. D.; Raghavachari, K.; Foresman, J. B.; Ortiz, J. V.; Cui, Q.; Baboul, A. G.; Clifford, S.; Cioslowski, J.; Stefanov, B. B.; Liu, G.; Liashenko, A.; Piskorz, P.; Komaromi, I.; Martin, R. L.; Fox, D. J.; Keith, T.; Al-Laham, M. A.; Peng, C. Y.; Nanayakkara, A.; Challacombe, M.; Gill, P. M. W.; Johnson, B.; Chen, W.; Wong, M. W.; Gonzalez, C.; Pople, J. A. *Gaussian03, Revision A.1*; Gaussian: Pittsburgh, PA, 2003.
19. (a) Roothan, C. C. J. *Rev. Mod. Phys.* **1951**, *23*, 69; (b) Pople, J. A.; Nesbet, R. K. *J. Chem. Phys.* **1954**, *22*, 571; (c) McWeeny, R.; Dierksen, G. *J. Chem. Phys.* **1968**, *49*, 4852.
20. (a) Binkley, J. S.; Pople, J. A.; Hehre, W. J. *J. Am. Chem. Soc.* **1980**, *102*, 939; (b) Gordon, M. S.; Binkley, J. S.; Pople, J. A.; Pietro, W. J.; Hehre, W. J. *J. Am. Chem. Soc.* **1982**, *104*, 2797; (c) Pietro, W. J.; Francl, M. M.; Hehre, W. J.; Defrees, D. J.; Pople, J. A.; Binkley, J. S. *J. Am. Chem. Soc.* **1982**, *104*, 5039; (d) Dobbs, K. D.; Hehre, W. J. *J. Comput. Chem.* **1986**, *7*, 359; (e) Dobbs, K. D.; Hehre, W. J. *J. Comput. Chem.* **1987**, *8*, 861; (f) Dobbs, K. D.; Hehre, W. J. *J. Comput. Chem.* **1987**, *8*, 880.
21. Mulliken, R. S. *J. Chem. Phys.* **1955**, *23*, 1833.
22. (a) Carpenter, J. E.; Weinhold, F. *J. Mol. Struct. (Theochem)* **1988**, *169*, 41; (b) Carpenter, J. E.. Ph.D. Thesis, University of Wisconsin, Madison, WI, 1987; (c) Foster, J. P.; Weinhold, F. *J. Am. Chem. Soc.* **1986**, *102*, 7211; (d) Reed, A. E.; Weinhold, F. *J. Chem. Phys.* **1983**, *78*, 4066; (e) Reed, A. E.; Weinhold, F. *J. Chem. Phys.* **1986**, 1736; (f) Reed, A. E.; Weinstock, R. B.; Weinhold, F. *J. Chem. Phys.* **1985**, *83*, 735; (g) Reed, A. E.; Curtiss, L. A.; Weinhold, F. *Chem. Rev.* **1988**, *88*, 899; (h) Weinhold, F.; Carpenter, J. E. *Plenum* **1988**, 227.
23. GaussView 3.0, Gaussian, Inc., Pittsburgh, PA, 2003.
24. Maruyama, T.; Ikeo, T.; Ueki, M. *Tetrahedron Lett.* **1999**, *40*, 5031–5034.
25. Ellman, G. L. *Arch. Biochem. Biophys.* **1959**, *82*, 70–77.
26. Artis, D. R.; Lipton, M. A. *J. Am. Chem. Soc.* **1998**, *120*, 12200–12206.
27. Baldauf, C.; Gunther, R.; Hofmann, H.-J. *J. Org. Chem.* **2004**, *69*, 6214–6220.